THE JOURNAL OF PHYSICAL CHEMISTRY C

Article

Cite This: J. Phys. Chem. C 2018, 122, 3256−3262

pubs.acs.org/JPCC

Nuclear Magnetic Resonance Study of Anion and Cation Reorientational Dynamics in $(NH_4)_2B_{12}H_{12}$

Alexander V. Skripov,*[,†] Roman V. Skoryunov,[†] Alexei V. Soloninin,[†] Olga A. Babanova,[†] Vitalie Stavila,[§] and Terrence J. Udovic[‡]

[†]Institute of Metal Physics, Ural Division of the Russian Academy of Sciences, S. Kovalevskoi 18, Ekaterinburg 620108, Russia

[§]Energy Nanomaterials, Sandia National Laboratories, Livermore, California 94551, United States

[‡]NIST Center for Neutron Research, National Institute of Standards and Technology, Gaithersburg, Maryland 20899-6102, United States

ABSTRACT: Diammonium dodecahydro-*closo*-dodecaborate $(NH_4)_2B_{12}H_{12}$ is the ionic compound combining NH_4^+ cations and $[B_{12}H_{12}]^{2-}$ anions, both of which can exhibit high reorientational mobility. To study the dynamical properties of this material, we measured the proton NMR spectra and spin−lattice relaxation rates in $(NH_4)_2B_{12}H_{12}$ over the temperature range of 6−475 K. Two reorientational processes occurring at different frequency scales have been revealed. In the temperature range of 200−475 K, the proton spin−lattice relaxation data are governed by thermally activated reorientations of the icosahedral $[B_{12}H_{12}]^{2-}$ anions. This motional process is characterized by the activation energy of 486(8) meV, and the corresponding reorientational jump rate reaches $\sim 10^8$ s^{-1} near 410 K. Below 100 K, the relaxation data are governed by the extremely fast process of NH_4^+ reorientations which are not "frozen out" at the NMR frequency scale down to 6 K. The experimental results in this range are described in terms of a gradual transition from the regime of low-temperature quantum dynamics (rotational tunneling of NH_4 groups) to the regime of classical jump reorientations of NH_4 groups with an activation energy of 26.5 meV. Our study offers physical insights into the rich dynamical behavior of $(NH_4)_2B_{12}H_{12}$ on an atomic level, providing a link between the microscopic and thermodynamic properties of this compound.

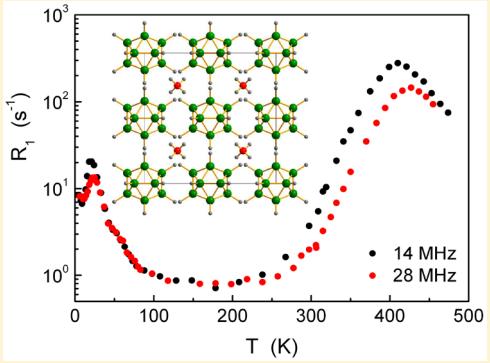

INTRODUCTION

The properties of *closo*-polyborates containing complex polyhedral $[B_{12}H_{12}]^{2-}$ and $[B_{10}H_{10}]^{2-}$ anions have received significant recent attention.[1−3] The original interest in these compounds was related to the formation of alkali-metal (A) and alkaline-earth (Ae) salts $A_2B_{12}H_{12}$ and $AeB_{12}H_{12}$ as stable intermediate products of dehydrogenation reactions of prospective hydrogen-storage materials—alkali-metal and alkaline-earth borohydrides.[4−6] Recently, it has been found that the disordered high-temperature phases of Li and Na *closo*-polyborates $A_2B_{12}H_{12}$ and $A_2B_{10}H_{10}$ (A = Li, Na) exhibit remarkable superionic conductivity.[7−9] Since the high A^+ conductivity in these phases is accompanied by extremely fast reorientational motion of $[B_{12}H_{12}]^{2-}$ and $[B_{10}H_{10}]^{2-}$ anions,[10−13] it is likely that the enhanced cation mobility is facilitated by reorientations of these large anions.[14,15]

By combining the $[B_{12}H_{12}]^{2-}$ anion with an H-containing cation, such as $[NH_4]^+$, one may expect to form a potentially useful hydrogen-storage material with high H content. Indeed, the diammonium dodecahydro-*closo*-dodecaborate, $(NH_4)_2B_{12}H_{12}$, with the H content of 11.3 wt % is known to exist as a stable cubic compound (space group $Fm\bar{3}$),[16] see Figure 1. Furthermore, ab initio DFT calculations[17] predict favorable thermodynamics for hydrogen release from this compound. $(NH_4)_2B_{12}H_{12}$ is isostructural with the cubic alkali-metal salts $K_2B_{12}H_{12}$, $Rb_2B_{12}H_{12}$, and $Cs_2B_{12}H_{12}$,[16] and its lattice parameter (a = 10.8781 Å)[16] is close to that for $Rb_2B_{12}H_{12}$ (10.8674 Å). Reorientational motion of large anions strongly contributes to the balance of energies determining the thermodynamic stability of complex hydrides. Therefore, information on the reorientational dynamics is important for understanding the fundamental properties of these compounds, including the nature and the mechanisms of phase transitions and hydrogen desorption. Microscopic information on H jump motion can be obtained from nuclear magnetic resonance (NMR) and quasielastic neutron scattering (QENS) measurements. Studies of the ^{11}B NMR spectra in the isomorphous cubic dodecahydro-*closo*-dodecaborates[18] have shown that the reorientational jump rate τ^{-1} of $[B_{12}H_{12}]^{2-}$ anions at a given temperature increases with increasing cation radius. However, such NMR spectral measurements can trace the atomic jump rate variations over rather limited dynamic ranges (usually not exceeding 2 orders of magnitude); this may lead to unreliable values of the motional parameters (activation energies and pre-

Received: December 7, 2017
Revised: January 26, 2018
Published: January 29, 2018

DOI: 10.1021/acs.jpcc.7b12046
J. Phys. Chem. C 2018, 122, 3256−3262

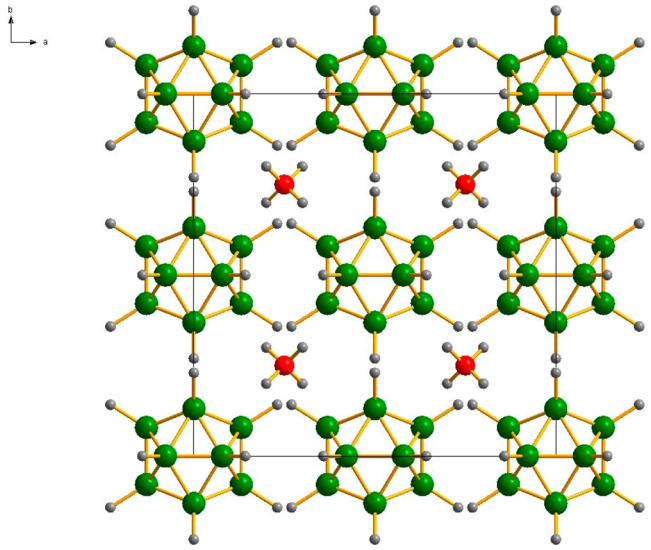

Figure 1. Schematic view of the structure of $(NH_4)_2B_{12}H_{12}$: (red spheres) N atoms; (green spheres) B atoms; (gray spheres) H atoms.

exponential factors τ_0^{-1} for the jump rates). In contrast, NMR measurements of the nuclear spin−lattice relaxation rates can trace changes in τ^{-1} over much broader dynamic ranges (up to 8 orders of magnitude for some alkali-metal borohydrides[19,20]). Such a broad dynamic range is expected to result in the high accuracy of the activation energies derived from the nuclear spin−lattice relaxation measurements. ^{1}H and ^{11}B spin−lattice relaxation measurements were used to determine the rates of $[B_{12}H_{12}]^{2-}$ reorientations in the cubic $A_2B_{12}H_{12}$ (A = K, Rb, Cs) compounds over wide temperature ranges.[10] However, the dynamics of $[B_{12}H_{12}]^{2-}$ anions in $(NH_4)_2B_{12}H_{12}$ has not been studied by NMR relaxometry so far. It should also be noted that the reorientational motion of $[B_{12}H_{12}]^{2-}$ in $(NH_4)_2B_{12}H_{12}$ cannot be easily studied by QENS, since the corresponding jump rates are expected to reach the QENS frequency "window" ($\tau^{-1} > 10^9$ s^{-1}) only above ∼500 K, not far from the onset of decomposition (∼610 K).[21]

Apart from the anion reorientations in $(NH_4)_2B_{12}H_{12}$, one may expect significant cation dynamics, since the ammonium groups in many compounds are known to exhibit fast rotational motion, including low-temperature rotational tunneling.[22−25] For $(NH_4)_2B_{12}H_{12}$, the low-temperature tunneling splitting of 18.5 μeV has been revealed by high-resolution inelastic neutron scattering measurements.[21] This splitting appears to be considerably larger than that observed for other ammonium-based systems.[22−25] The rotational tunneling peaks in $(NH_4)_2B_{12}H_{12}$ are found to persist up to 40 K; at higher temperatures, the neutron scattering spectra are dominated by the classical quasielastic contribution that can be attributed to NH_4^+ jump reorientations.[21] Thus, $(NH_4)_2B_{12}H_{12}$ is a system showing very rich dynamical behavior at different frequency scales. NMR measurements of the spin−lattice relaxation rates at low temperatures may complement QENS measurements, since NMR data are sensitive to much slower hydrogen motions.[26] Furthermore, from the methodological point of view, comparison of the tunneling parameters derived from neutron scattering and NMR may help to develop approaches to complex interpretations of the experimental data in systems with rotational tunneling.[25] The aim of the present work is to investigate the dynamics of both $[B_{12}H_{12}]^{2-}$ anions and $[NH_4]^+$ cations in $(NH_4)_2B_{12}H_{12}$ using proton spin−lattice relaxation rate measurements over a wide temperature range (6−475 K).

EXPERIMENTAL METHODS

Preparation of the powdered $(NH_4)_2B_{12}H_{12}$ sample was analogous to that described in ref 21. For NMR experiments, the samples were flame sealed in glass tubes under vacuum. Proton NMR measurements were performed on a pulse spectrometer with quadrature phase detection at frequencies $\omega/2\pi$ = 14 and 28 MHz. The magnetic field was provided by a 2.1 T iron-core Bruker magnet. A home-built multinuclear continuous-wave NMR magnetometer working in the range 0.32−2.15 T was used for field stabilization. For rf pulse generation, we used a home-built computer-controlled pulse programmer, the PTS frequency synthesizer (Programmed Test Sources, Inc.[27]), and a 1 kW Kalmus wideband pulse amplifier. Typical values of the $\pi/2$ pulse length were 2−3 μs. A probehead with the sample was placed into an Oxford Instruments CF1200 continuous-flow cryostat using helium or nitrogen as a cooling agent. The sample temperature, monitored by a chromel-(Au−Fe) thermocouple, was stable to ±0.1 K. The nuclear spin−lattice relaxation rates were measured using the saturation−recovery method. NMR spectra were recorded by Fourier transforming the solid echo signals (pulse sequence $\pi/2_x - t - \pi/2_y$).

For all figures, standard uncertainties are commensurate with the observed scatter in the data, if not explicitly designated by vertical error bars.

RESULTS AND DISCUSSION

Overview. The temperature dependences of the proton spin−lattice relaxation rates R_1 measured at two resonance frequencies $\omega/2\pi$ for $(NH_4)_2B_{12}H_{12}$ are shown in Figure 2. As

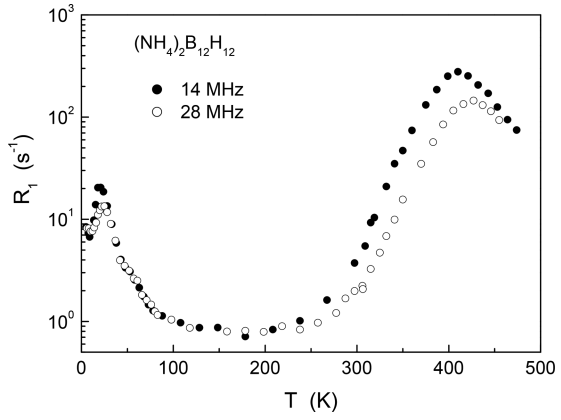

Figure 2. Temperature dependences of the proton spin−lattice relaxation rates measured at 14 and 28 MHz for $(NH_4)_2B_{12}H_{12}$.

can be seen from this figure, $R_1(T)$ exhibits two frequency-dependent peaks. General features of the observed behavior of R_1 in the regions of each of the peaks are typical of a relaxation mechanism due to nuclear dipole−dipole interaction modulated by atomic motion.[28] For this mechanism, the $R_1(T)$ peak is expected to occur at the temperature at which the atomic jump rate $\tau^{-1}(T)$ becomes nearly equal to ω. The presence of two well-separated $R_1(T)$ peaks indicates a coexistence of two types of atomic motion with strongly differing characteristic jump rates; for the faster motion, the peak should be observed at lower temperature. Comparison of the $R_1(T)$ results

DOI: 10.1021/acs.jpcc.7b12046
J. Phys. Chem. C 2018, 122, 3256−3262

presented in Figure 2 with the corresponding data[10] for cubic $K_2B_{12}H_{12}$, $Rb_2B_{12}H_{12}$, and $Cs_2B_{12}H_{12}$ suggests that the high-temperature relaxation rate peak for $(NH_4)_2B_{12}H_{12}$ originates from the reorientational motion of the $[B_{12}H_{12}]^{2-}$ anions. The low-temperature $R_1(T)$ peak for $(NH_4)_2B_{12}H_{12}$ should then be attributed to the much faster reorientational motion of the $[NH_4]^+$ cations. This assignment is supported by the behavior of the ^{1}H NMR spectra, to be discussed below. It should be noted that the low-T relaxation rate peak is observed near 20 K; this indicates that $[NH_4]^+$ groups participate in extremely fast motion even at very low temperatures.

In the temperature range between the two peaks, the $R_1(T)$ data are governed by another (background) relaxation mechanism. A possible background relaxation mechanism may be related to spin diffusion to paramagnetic impurities.[29]

Figure 3 shows the evolution of the measured ^{1}H NMR spectra for $(NH_4)_2B_{12}H_{12}$ with temperature. It can be seen that

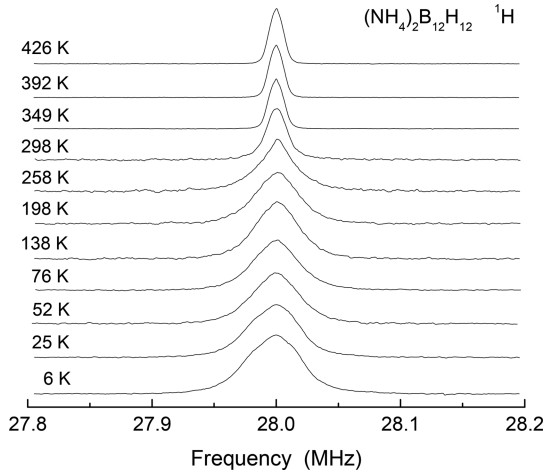

Figure 3. Evolution of the measured ^{1}H NMR spectra with temperature for $(NH_4)_2B_{12}H_{12}$.

both the shape and the width of the proton NMR spectrum are temperature dependent, and the line width decreases with increasing temperature. Such a behavior can be attributed to a partial averaging of the dipole−dipole interactions of ^{1}H spins due to atomic motion. The motional narrowing is expected to be substantial at the temperature at which the H jump rate $\tau^{-1}(T)$ becomes comparable to the "rigid lattice" line width $\Delta\nu_R$;[28] for typical complex hydrides, $\Delta\nu_R$ is of the order of 10^4−10^5 s^{-1}.

The temperature dependence of the measured ^{1}H line width $\Delta\nu$ (full width at half-maximum) is shown in Figure 4. As can be seen from this figure, $\Delta\nu(T)$ exhibits two plateau regions (for temperatures between 60 and 200 K and above 350 K). Such plateau regions are typical of reorientational motion of H-containing groups.[30] In contrast to long-range translational diffusion that leads to complete averaging of the dipole−dipole interactions of ^{1}H spins, the averaging due to reorientational motion is only partial. It is usually assumed that for $\tau^{-1} \gg 2\pi\Delta\nu_R$, the dipole−dipole interactions within the reorienting groups ("intramolecular" interactions) are completely averaged out, while the interactions between ^{1}H spins on different groups ("intermolecular" interactions) are not averaged.

In order to interpret the observed proton line widths at different temperatures, it is useful to calculate the second moments of the ^{1}H NMR spectra. On the basis of the structural

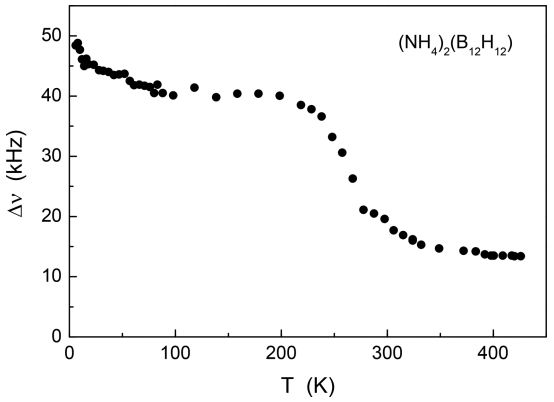

Figure 4. Temperature dependence of the width (full width at half-maximum) of the ^{1}H NMR line measured at 28 MHz for $(NH_4)_2B_{12}H_{12}$.

data for $(NH_4)_2B_{12}H_{12}$,[21] we calculated the "rigid lattice" second moment of the ^{1}H NMR line using the standard Van Vleck formalism[28] and taking into account the ^{1}H−^{1}H, ^{1}H−^{11}B, ^{1}H−^{10}B, and ^{1}H−^{14}N dipole−dipole interactions: $M_2^R = 4.15 \times 10^{10}$ s^{-2}. It should be noted that this value is dominated by ^{1}H−^{1}H and ^{1}H−^{11}B interactions, which are responsible for 96% of the calculated M_2^R. Assuming a Gaussian shape of the proton NMR line, the calculated M_2^R value should correspond to $\Delta\nu$ = 76.5 kHz. The experimental $\Delta\nu$ value at 6 K is considerably smaller (48 kHz); this suggests that even at the lowest temperature, a certain part of the dipole−dipole interaction is averaged out. Similar results were recently reported for the ^{1}H line width in $Sr(BH_4)_2(NH_3)_2$.[31] Such a behavior of the low-temperature proton NMR line width is typical of the case of rotational tunneling.[32] The expected value of $\Delta\nu$ at the high-temperature plateau can be roughly estimated in the following way. Since fast rotational motion should average out the dipole−dipole interactions within the rotating quasi-spherical group, we have to calculate only the dipolar interactions between different rotating groups. Such an "intermolecular" contribution to the second moment can be estimated by placing all of the nuclear spins of the group at its center and taking into account only the distances between centers of different groups.[33] In the following estimates we take into account only the dominant ^{1}H−^{1}H and ^{1}H−^{11}B interactions. For fast rotations of both NH_4 and $B_{12}H_{12}$ groups in $(NH_4)_2B_{12}H_{12}$, we obtain a second moment of 1.33×10^9 s^{-2}. For a Gaussian shape of the proton NMR line, this value corresponds to a line width of 13.7 kHz, in excellent agreement with the observed $\Delta\nu$ at the high-temperature plateau (13.5 kHz). For fast rotations of NH_4 groups and static $B_{12}H_{12}$ groups, we obtain a second moment of 1.36×10^{10} s^{-2}, which corresponds to a line width of 43.7 kHz. This value is close to the observed $\Delta\nu$ (~40 kHz) at the intermediate plateau between 60 and 200 K (see Figure 4). Thus, our ^{1}H NMR line width results support the assignment of the proton spin−lattice relaxation rate peaks: the low-temperature $R_1(T)$ peak is associated with the motion of NH_4 groups, while the high-temperature one is related to the motion of $B_{12}H_{12}$ groups.

High-Temperature Region: $B_{12}H_{12}$ Reorientations. First, we shall discuss the behavior of the proton spin−lattice relaxation rates in the region of the high-temperature peak. Figure 5 shows the measured spin−lattice relaxation rates in this region as a function of the inverse temperature.

DOI: 10.1021/acs.jpcc.7b12046
J. Phys. Chem. C 2018, 122, 3256−3262

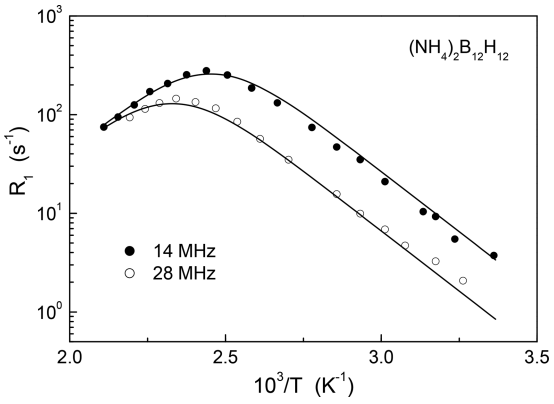

Figure 5. Proton spin−lattice relaxation rates measured at 14 and 28 MHz in the region of the high-temperature peak as a function of the inverse temperature. Solid lines show the simultaneous fit of the standard model to the data.

According to the standard theory of nuclear spin−lattice relaxation due to the motionally-modulated dipole−dipole interaction,[28] in the limit of slow motion ($\omega\tau \gg 1$), R_1 should be proportional to $\omega^{-2}\tau^{-1}$, and in the limit of fast motion ($\omega\tau \ll 1$), R_1 should be proportional to τ being frequency independent. If the temperature dependence of the jump rate τ^{-1} follows the Arrhenius law

$$\tau^{-1} = \tau_0^{-1} \exp(-E_a/k_B T) \quad (1)$$

with the activation energy E_a, the plot of ln R_1 versus T^{-1} is expected to be linear in the limits of both slow and fast motion with slopes of $-E_a/k_B$ and E_a/k_B, respectively. As can be seen from Figure 5, the experimental data in the region of the high-temperature peak are consistent with these predictions. In particular, we have not found any signs of distributions of the jump rates, which would have led to certain deviations[34] from these predictions. Thus, for parametrization of the $R_1(T)$ data in the region of the high-temperature peak we used the Arrhenius law and the standard relation between R_1 and τ

$$R_1 = \frac{\Delta M_{HB}}{2}\left[\frac{\tau}{1+(\omega_H-\omega_B)^2\tau^2} + \frac{3\tau}{1+\omega_H^2\tau^2} + \frac{6\tau}{1+(\omega_H+\omega_B)^2\tau^2}\right] + \frac{2\Delta M_{HH}}{3}\left[\frac{\tau}{1+\omega_H^2\tau^2} + \frac{4\tau}{1+4\omega_H^2\tau^2}\right] \quad (2)$$

where ω_H and ω_B are the resonance frequencies of ^{1}H and ^{11}B, respectively, and ΔM_{HB} and ΔM_{HH} are the parts of the dipolar second moment due to ^{1}H−^{11}B and ^{1}H−^{1}H interactions that are caused to fluctuate by the reorientational motion. Here we neglect ^{1}H−^{10}B and ^{1}H−^{14}N interactions, since our calculations (see above) show that these interactions are responsible for about 4% of the total second moment. Furthermore, because the ^{1}H−^{11}B and ^{1}H−^{1}H terms in eq 2 show nearly the same temperature and frequency dependences, it is practically impossible to determine both amplitude parameters ΔM_{HB} and ΔM_{HH} independently from the fits. Therefore, we have to assume that the ratio $\Delta M_{HB}/\Delta M_{HH}$ is the same as for the corresponding contributions to the "rigid lattice" second moment; this calculated ratio is 0.23. The fit parameters are the activation energy E_a, the pre-exponential factor τ_0 in the Arrhenius law, and the single amplitude parameter ΔM_{HH}. These parameters have been varied to find the best fit to the $R_1(T)$ data at two resonance frequencies *simultaneously*. The results of the simultaneous fit over the T range of 297−474 K are shown by solid lines in Figure 5; the corresponding parameters are E_a = 486(8) meV, τ_0 = 1.1(1) × 10^{-14} s, and ΔM_{HH} = 1.6(1) × 10^{10} s^{-2}. Note that the value of ΔM_{HH} resulting from the fit is considerably smaller than the calculated ^{1}H−^{1}H contribution to the "rigid lattice" second moment, 3.26 × 10^{10} s^{-2}. This is typical of the case of localized H motion. It should also be noted that our E_a value for $B_{12}H_{12}$ reorientations in $(NH_4)_2B_{12}H_{12}$ is considerably smaller than that obtained from changes in the ^{11}B NMR line width (930 meV).[18] As discussed previously,[10] all of the activation energies derived from the ^{11}B NMR spectra in ref 18 appear to be strongly overestimated. An additional indication of the overestimated E_a value for $(NH_4)_2B_{12}H_{12}$ in ref 18 is the unreasonably small value of the pre-exponential factor τ_0 (6.2 × 10^{-22} s) obtained in this work. Such a small value of τ_0 is difficult to justify.

The activation energies for $B_{12}H_{12}$ reorientations derived from the proton spin−lattice relaxation measurements in the isomorphous cubic $A_2B_{12}H_{12}$ compounds are compared in Table 1.

Included in Table 1 are also the lattice parameters, the temperatures of the $R_1(T)$ maxima, T_{max}, at $\omega/2\pi$ = 14 MHz, and the temperature ranges over which the $R_1(T)$ data were analyzed. The values of T_{max} correspond to the temperatures at which the jump rate τ^{-1} becomes nearly equal to $\omega \approx 10^8$ s^{-1}; thus, they can be used to compare the jump rates in different compounds: for compounds with faster motion, T_{max} should be lower. It can be seen from Table 1 that the reorientational motion of $B_{12}H_{12}$ groups in $(NH_4)_2B_{12}H_{12}$ is consistent with the general trends for the cubic alkali-metal *closo*-dodecaborates: with increasing lattice parameter, the motion becomes faster and its activation energy becomes smaller.

Low-Temperature Region: NH_4 Motion. The behavior of the proton spin−lattice relaxation rates in the region of the low-temperature peak is shown in Figure 6.

A standard interpretation of this peak in terms of thermally activated reorientational motion would mean that the H jump motion reaches ~10^8 s^{-1} at 20 K. However, a closer inspection

Table 1. Temperatures of the $R_1(T)$ Maxima at 14 MHz and Activation Energies for Anion Reorientations in $A_2B_{12}H_{12}$ (A = K, Rb, NH_4, Cs)[a]

compound	lattice parameter[b] a (Å)	T_{max} (K)	activation energy E_a (meV)	temperature range for E_a fits (K)	ref
$K_2B_{12}H_{12}$	10.6290 (8)	490 (5)	800 (11)	366−564	10
$Rb_2B_{12}H_{12}$	10.8674 (8)	417 (3)	549 (5)	315−560	10
$(NH_4)_2B_{12}H_{12}$	10.8781 (9)	410 (3)	486 (8)	297−474	this work
$Cs_2B_{12}H_{12}$	11.2812 (7)	365 (3)	427 (4)	260−570	10

[a]Uncertainties in the last digit are given in parentheses. [b]From ref 16.

DOI: 10.1021/acs.jpcc.7b12046
J. Phys. Chem. C 2018, 122, 3256−3262

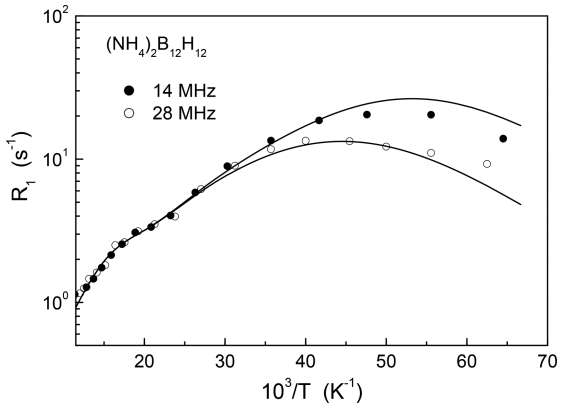

Figure 6. Proton spin−lattice relaxation rates measured at 14 and 28 MHz in the region of the low-temperature peak as a function of the inverse temperature. Solid lines show the simultaneous fit of the model based on eqs 3 and 4 to the data.

of the data in Figure 6 reveals significant deviations from the standard behavior. In particular, the frequency-independent "shoulder" can be seen near 50 K at the high-temperature slope of the peak. Such a feature of the $R_1(T)$ data is considered as a characteristic sign of rotational tunneling[32,35] when the tunneling splitting of the ground state exceeds the Zeeman splitting of the nuclear spin levels. Similar $R_1(T)$ "shoulders" were observed earlier for a number of systems exhibiting rotational tunneling of methyl groups.[32,35−37] However, for ammonium groups, this $R_1(T)$ feature has not been reported so far; its appearance for $(NH_4)_2B_{12}H_{12}$ may be related to the unusually large tunnel splitting revealed for this compound by inelastic neutron scattering.[21]

The usual approach to the description of rotational tunneling effects on the proton spin−lattice relaxation governed by fluctuating dipole−dipole interactions is based on the model introduced by Haupt.[35] The corresponding expression for R_1 is

$$R_1 = C_1 \sum_{n=-2}^{2} \frac{n^2\tau_c}{1 + (\omega_t + n\omega)^2\tau_c^2} + C_2 \sum_{n=1}^{2} \frac{n^2\tau_c}{1 + n^2\omega^2\tau_c^2} \quad (3)$$

The first term in eq 3 with the relaxation strength C_1 arises from fluctuations of the "intramolecular" dipole−dipole interactions due to transitions between the tunneling-split states of the rotor. This term contains the tunneling frequency ω_t that determines the splitting, $\hbar\omega_t$. If ω_t is much larger than the resonance (Larmor) frequency ω, the first term becomes ω independent. The second term with the relaxation strength C_2 arises from fluctuations of the "intermolecular" dipole−dipole interactions; the form of this term corresponds to the classical expression for R_1. The correlation time τ_c for dipole−dipole interactions is determined by the lifetime of the tunneling states at low temperatures and by the mean H residence times at high temperatures; the temperature dependence of τ_c is usually approximated as[36]

$$\tau_c^{-1} = \tau_{01}^{-1} \exp(-E_{01}/k_BT) + \tau_{02}^{-1} \exp(-E_{a2}/k_BT) \quad (4)$$

Here E_{01} is the energy difference between the librational ground and the first excited state and E_{a2} is the classical activation energy related to the potential barrier height. For parametrization of the experimental $R_1(T)$ data in the region of the low-temperature peak, we used the model based on eqs 3 and 4. The fit parameters (C_1, C_2, ω_t, E_{01}, E_{a2}, τ_{01}, and τ_{02}) have been varied to find the best fit to the $R_1(T)$ data at two resonance frequencies *simultaneously*. The results of the simultaneous fit over the T range of 15.5−83 K are shown by solid lines in Figure 6; the corresponding parameters are $C_1 = 2.3 \times 10^9\ s^{-2}$, $C_2 = 1.6 \times 10^9\ s^{-2}$, $\omega_t = 7.7 \times 10^9\ s^{-1}$, $E_{01} = 7.0$ meV, $E_{a2} = 26.5$ meV, $\tau_{01} = 9.3 \times 10^{-11}$ s, and $\tau_{02} = 1.0 \times 10^{-12}$ s. The temperature dependence of the inverse correlation time τ_c^{-1} resulting from this fit is shown in Figure 7. This plot demonstrates a smooth transition from quantum dynamics at low temperatures to classical behavior at higher temperatures.

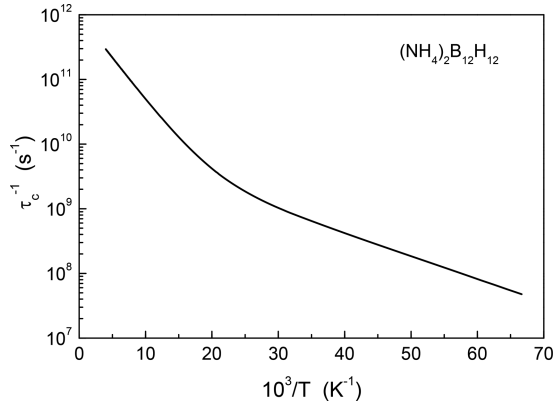

Figure 7. Temperature dependence of the inverse correlation time τ_c^{-1} for NH_4 groups resulting from the low-temperature spin−lattice relaxation fit.

In energy units, the value of ω_t resulting from our fit corresponds to 5.1 μeV. For tetrahedral symmetry, the librational ground level is split into three rotational states denoted as A, T, and E.[25] The T−E rotational tunnel splitting of the ground state for $(NH_4)_2B_{12}H_{12}$ obtained from inelastic neutron scattering (INS) measurements at 4 K is 18.5 μeV.[21] However, the tunnel splitting strongly decreases with increasing temperature, and at 40 K it drops to ∼8 μeV.[21] Following the approach of ref 36, we have not tried to take the temperature dependence of ω_t into account, since this would require additional fit parameters. Attempts to include an empirical temperature dependence of ω_t do not lead to any significant changes in the effective activation energies E_{01} and E_{a2}. Therefore, the value of ω_t in eq 3 should be considered as the "average" tunneling frequency;[36] its contribution to $R_1(T)$ is the strongest at the temperature of the "shoulder" (∼50 K) corresponding to $\omega_t\tau_c = 1$. Hence, the value of $\hbar\omega_t$ resulting from the $R_1(T)$ fits is expected to be considerably smaller than the low-T limit of the tunnel splitting observed by INS. This is what is found in our case; similar results were also obtained for a number of systems with rotational tunneling of methyl groups.[36]

The value of E_{01} resulting from our fit (7.0 meV) appears to be close to the 7.8 meV INS peak[21] assigned to the transition between the ground and the first excited librational states of the NH_4 group. Therefore, the low-temperature behavior of $R_1(T)$ is consistent with changes in the lifetimes of the ground librational states. The value of E_{a2} resulting from our fit should be compared to the quasielastic neutron scattering (QENS) results[21] describing the temperature dependence of the H jump rate for NH_4 groups in $(NH_4)_2B_{12}H_{12}$ in the classical limit. The QENS line width data of ref 21 over the temperature range of ∼70−200 K correspond to an effective activation energy of 24.5

DOI: 10.1021/acs.jpcc.7b12046
J. Phys. Chem. C 2018, 122, 3256−3262

meV. This value is close to our E_{a2} result (26.5 meV). Thus, the main parameters derived from our analysis of the low-temperature proton spin−lattice relaxation data are consistent with the neutron scattering results.[21] This justifies the use of the model description of NMR data based on eqs 3 and 4 and suggests that both NMR and neutron scattering can be employed as complementary methods for studies of the low-temperature NH_4 dynamics.

It should be noted that $[B_{12}H_{12}]^{2-}$ appears to be the largest counterion for ammonium salts where NH_4 dynamics has been studied. One may expect that the large size of $[B_{12}H_{12}]^{2-}$ anions is one of the main factors responsible for the soft ammonium rotational potential in the crystal lattice of $(NH_4)_2B_{12}H_{12}$. In fact, relatively loose coordination of NH_4 groups in large interstitial sites of the *fcc* sublattice of $[B_{12}H_{12}]^{2-}$ anions may lead to low barriers for ammonium rotations. Low rotational barriers should correspond to high values of the tunnel splitting $\hbar\omega_t$ and to low values of the activation energy E_{a2}. For $(NH_4)_2B_{12}H_{12}$, the low-temperature $\hbar\omega_t$ values (18.5 and 37 μeV for the T−E and A−T rotational transitions, respectively)[21] are indeed considerably larger than those for other ammonium salts studied, e.g., 1.09 μeV for $(NH_4)_2S_2O_8$,[25] 5.65 μeV for NH_4ClO_4,[23] and 0.21 μeV for $(NH_4)_2ZnCl_4$.[38] Furthermore, the value of the activation energy E_{a2} for classical NH_4 reorientations in $(NH_4)_2B_{12}H_{12}$ (26.5 meV) is smaller than the corresponding values found in other ammonium salts, e.g., 40 meV for $(NH_4)_2S_2O_8$,[25] 31 meV for NH_4ClO_4,[39] and 95 meV for NH_4ReO_4.[39] Thus, the values of both ω_t and E_{a2} for $(NH_4)_2B_{12}H_{12}$ are consistent with very low barriers for ammonium rotations in this compound.

CONCLUSIONS

Analysis of the temperature and frequency dependences of the ^1H spin−lattice relaxation rate in the diammonium dodecahydro-*closo*-dodecaborate $(NH_4)_2B_{12}H_{12}$ has revealed a coexistence of two reorientational processes occurring at different frequency scales. In the temperature range of 200−475 K, the relaxation data are governed by thermally activated reorientations of the icosahedral $[B_{12}H_{12}]^{2-}$ anions. This motional process is characterized by the activation energy of 486(8) meV, and the corresponding reorientational jump rate reaches $\sim 10^8$ s^{-1} near 410 K. The parameters of $B_{12}H_{12}$ reorientations in $(NH_4)_2B_{12}H_{12}$ are consistent with the general trends for the cubic alkali-metal *closo*-dodecaborates: with increasing lattice parameter, the motion becomes faster and its activation energy becomes smaller. Below 100 K, the proton spin−lattice relaxation data are governed by the extremely fast process of $[NH_4]^+$ reorientations which are not "frozen out" at the NMR frequency scale down to 6 K. The experimental results in this range are described in terms of a gradual transition from the regime of low-temperature quantum dynamics (rotational tunneling of NH_4 groups) to the regime of classical jump reorientations of NH_4 groups with an activation energy of 26.5 meV at higher temperatures. Comparison of our low-temperature results with those of inelastic neutron scattering study[21] indicates that both NMR and neutron scattering can be used as complementary methods for studies of different regimes of extremely fast NH_4 dynamics in $(NH_4)_2B_{12}H_{12}$. The motional parameters derived from our experiments suggest low barriers for NH_4 rotations in $(NH_4)_2B_{12}H_{12}$; this is consistent with the large anion/cation size ratio for this compound.

AUTHOR INFORMATION

Corresponding Author

*E-mail: skripov@imp.uran.ru. Fax: +7-343-374-5244.

ORCID

Alexander V. Skripov: 0000-0002-0610-5538

Notes

The authors declare no competing financial interest.

ACKNOWLEDGMENTS

This work was carried out within the assignment of the Russian Federal Agency of Scientific Organizations (program "Spin" No. 01201463330), supported in part by the Russian Foundation for Basic Research (Grant No. 15-03-01114). Sandia National Laboratories is a multimission laboratory managed and operated by National Technology and Engineering Solutions of Sandia, LLC., a wholly owned subsidiary of Honeywell International, Inc., for the US Department of Energy's National Nuclear Security Administration under contract DE-NA-0003525.

REFERENCES

(1) Paskevicius, M.; Jepsen, L. H.; Schouwink, P.; Černý, R.; Ravnsbæk, D. B.; Filinchuk, Y.; Dornheim, M.; Besenbacher, F.; Jensen, T. R. Metal Borohydrides and Derivatives − Synthesis, Structure and Properties. *Chem. Soc. Rev.* **2017**, *46*, 1565−1634.

(2) Mohtadi, R.; Orimo, S. The Renaissance of Hydrides as Energy Materials. *Nature Rev. Mater.* **2016**, *2*, 16091.

(3) Tang, W. S.; Dimitrievska, M.; Stavila, V.; Zhou, W.; Wu, H.; Talin, A. A.; Udovic, T. J. Order-Disorder Transitions and Superionic Conductivity in the Sodium Nido-Undeca(carba)borates. *Chem. Mater.* **2017**, *29*, 10496−10509.

(4) Orimo, S.; Nakamori, Y.; Ohba, N.; Miwa, K.; Aoki, M.; Towata, S.; Züttel, A. Experimental Studies on Intermediate Compound of $LiBH_4$. *Appl. Phys. Lett.* **2006**, *89*, 021920.

(5) Hwang, S.-J.; Bowman, R. C.; Reiter, J. W.; Rijssenbeek, J.; Soloveichik, G. L.; Zhao, J.-C.; Kabbour, H.; Ahn, C. C. NMR Confirmation for Formation of $[B_{12}H_{12}]^{2-}$ Complexes during Hydrogen Desorption from Metal Borohydrides. *J. Phys. Chem. C* **2008**, *112*, 3164−3169.

(6) Pitt, M. P.; Paskevicius, M.; Brown, D. H.; Sheppard, D. A.; Buckley, C. E. Thermal Stability of $Li_2B_{12}H_{12}$ and Its Role in the Decomposition of $LiBH_4$. *J. Am. Chem. Soc.* **2013**, *135*, 6930−6941.

(7) Udovic, T. J.; Matsuo, M.; Unemoto, A.; Verdal, N.; Stavila, V.; Skripov, A. V.; Rush, J. J.; Takamura, H.; Orimo, S. Sodium Superionic Conduction in $Na_2B_{12}H_{12}$. *Chem. Commun.* **2014**, *50*, 3750−3752.

(8) Udovic, T. J.; Matsuo, M.; Tang, W. S.; Wu, H.; Stavila, V.; Soloninin, A. V.; Skoryunov, R. V.; Babanova, O. A.; Skripov, A. V.; Rush, J. J.; et al. Exceptional Superionic Conductivity in Disordered Sodium Decahydro-*closo*-decaborate. *Adv. Mater.* **2014**, *26*, 7622−7626.

(9) Tang, W. S.; Matsuo, M.; Wu, H.; Stavila, V.; Unemoto, A.; Orimo, S.; Udovic, T. J. Stabilizing Lithium and Sodium Fast-Ion Conduction in Solid Polyhedral-Borate Salts at Device-Relevant Temperatures. *Energy Storage Mater.* **2016**, *4*, 79.

(10) Skripov, A. V.; Babanova, O. A.; Soloninin, A. V.; Stavila, V.; Verdal, N.; Udovic, T. J.; Rush, J. J. Nuclear Magnetic Resonance Study of Atomic Motion in $A_2B_{12}H_{12}$ (A = Na, K, Rb, Cs): Anion Reorientations and Na^+ Mobility. *J. Phys. Chem. C* **2013**, *117*, 25961−25968.

(11) Verdal, N.; Her, J.-H.; Stavila, V.; Soloninin, A. V.; Babanova, O. A.; Skripov, A. V.; Udovic, T. J.; Rush, J. J. Complex High-Temperature Phase Transitions in $Li_2B_{12}H_{12}$ and $Na_2B_{12}H_{12}$. *J. Solid State Chem.* **2014**, *212*, 81−90.

(12) Verdal, N.; Udovic, T. J.; Stavila, V.; Tang, W. S.; Rush, J. J.; Skripov, A. V. Anion Reorientations in the Superionic Conducting Phase of $Na_2B_{12}H_{12}$. *J. Phys. Chem. C* **2014**, *118*, 17483−17489.

DOI: 10.1021/acs.jpcc.7b12046
J. Phys. Chem. C 2018, 122, 3256−3262

(13) Soloninin, A. V.; Dimitrievska, M.; Skoryunov, R. V.; Babanova, O. A.; Skripov, A. V.; Tang, W. S.; Stavila, V.; Orimo, S.-c.; Udovic, T. J. Comparison of Anion Reorientational Dynamics in MCB_9H_{10} and $M_2B_{10}H_{10}$ (M = Li, Na) via Nuclear Magnetic Resonance and Quasielastic Neutron Scattering Studies. *J. Phys. Chem. C* **2017**, *121*, 1000−1012.
(14) Lu, Z.; Ciucci, F. Structural Origin of the Superionic Na Conduction in $Na_2B_{10}H_{10}$ *Closo*-Borates and Enhanced Conductivity by Na Deficiency for High Performance Solid Electrolyte. *J. Mater. Chem. A* **2016**, *4*, 17740−17748.
(15) Varley, J. B.; Kweon, K.; Mehta, P.; Shea, P.; Heo, T. W.; Udovic, T. J.; Stavila, V.; Wood, B. C. Understanding Ionic Conductivity Trends in Polyborane Solid Electrolytes from *Ab Initio* Molecular Dynamics. *ACS Energy Lett.* **2017**, *2*, 250−255.
(16) Tiritiris, I.; Schleid, T. Die Dodekahydro-*closo*-Dodekaborate $M_2[B_{12}H_{12}]$ der Schweren Alkalimetalle (M^+ = K^+, Rb^+, NH_4^+, Cs^+) und Ihre Formalen Iodid-Addukte $M_3I[B_{12}H_{12}]$ (≡ MI × $M_2[B_{12}H_{12}]$). *Z. Anorg. Allg. Chem.* **2003**, *629*, 1390−1402.
(17) Sun, W. Q.; Wolverton, C.; Akbarzadeh, A. R.; Ozolins, V. First-Principles Prediction of High-Capacity, Thermodynamically Reversible Hydrogen Storage Reactions Based on $(NH_4)_2B_{12}H_{12}$. *Phys. Rev. B: Condens. Matter Mater. Phys.* **2011**, *83*, 064112.
(18) Tiritiris, I.; Schleid, T.; Müller, K. Solid-State NMR Studies on Ionic *closo*-Dodecaborates. *Appl. Magn. Reson.* **2007**, *32*, 459−481.
(19) Babanova, O. A.; Soloninin, A. V.; Stepanov, A. P.; Skripov, A. V.; Filinchuk, Y. Structural and Dynamical Properties of $NaBH_4$ and KBH_4: NMR and Synchrotron X-ray Diffraction Studies. *J. Phys. Chem. C* **2010**, *114*, 3712−3718.
(20) Skripov, A. V.; Soloninin, A. V.; Babanova, O. A. Nuclear Magnetic Resonance Studies of Atomic Motion in Borohydrides. *J. Alloys Compd.* **2011**, *509*, S535−S539.
(21) Verdal, N.; Udovic, T. J.; Rush, J. J.; Stavila, V.; Wu, H.; Zhou, W.; Jenkins, T. Low-Temperature Tunneling and Rotational Dynamics of the Ammonium Cations in $(NH_4)_2B_{12}H_{12}$. *J. Chem. Phys.* **2011**, *135*, 094501.
(22) Prager, M.; Press, W.; Alefeld, B.; Hüller, A. Rotational States of the NH_4^+ Ion in $(NH_4)_2SnCl_6$ by Inelastic Neutron Scattering. *J. Chem. Phys.* **1977**, *67*, 5126−5132.
(23) Prager, M.; Press, W. Rotational Tunneling in NH_4ClO_4: Reanalysis of Neutron Spectra. *J. Chem. Phys.* **1981**, *75*, 494−495.
(24) Prager, M.; Heidemann, A. Rotational Tunneling and Neutron Spectroscopy: A Compilation. *Chem. Rev.* **1997**, *97*, 2933−2966.
(25) Prager, M.; Grimm, H.; Natkaniec, I.; Nowak, D.; Unruh, T. The Dimensionality of Ammonium Reorientation in $(NH_4)_2S_2O_8$: The View from Neutron Spectroscopy. *J. Phys.: Condens. Matter* **2008**, *20*, 125218.
(26) Skripov, A. V.; Shelyapina, M. G. In *Neutron Scattering and Other Nuclear Techniques for Hydrogen in Materials*; Fritzsche, H., Huot, J., Fruchart, D., Eds.; Springer International Publishing: Switzerland, 2016; pp 337−376.
(27) The mention of all commercial suppliers in this paper is for clarity and does not imply the recommendation or endorsement of these suppliers by NIST.
(28) Abragam, A. *The Principles of Nuclear Magnetism*; Clarendon Press: Oxford, 1961.
(29) Phua, T. T.; Beaudry, B. J.; Peterson, D. T.; Torgeson, D. R.; Barnes, R. G.; Belhoul, M.; Styles, G. A.; Seymour, E. F. W. Paramagnetic Impurity Effects in NMR Determinations of Hydrogen Diffusion and Electronic Structure in Metal Hydrides. Gd^{3+} in YH_2 and $LaH_{2.25}$. *Phys. Rev. B: Condens. Matter Mater. Phys.* **1983**, *28*, 6227−6250.
(30) Skripov, A. V.; Soloninin, A. V.; Babanova, O. A.; Skoryunov, R. V. Nuclear Magnetic Resonance Studies of Atomic Motion in Borohydride-Based Materials: Fast Anion Reorientations and Cation Diffusion. *J. Alloys Compd.* **2015**, *645*, S428−S433.
(31) Gradišek, A.; Jepsen, L. H.; Jensen, T. R.; Conradi, M. S. Nuclear Magnetic Resonance Study of Molecular Dynamics in Ammine Metal Borohydride $Sr(BH_4)_2(NH_3)_2$. *J. Phys. Chem. C* **2016**, *120*, 24646−24654.
(32) Horsewill, A. J. Quantum Tunnelling Aspects of Methyl Group Rotation Studied by NMR. *Prog. Nucl. Magn. Reson. Spectrosc.* **1999**, *35*, 359−389.
(33) Sorte, E. G.; Emery, S. B.; Majzoub, E. H.; Ellis-Caleo, T.; Ma, Z. L.; Hammann, B. A.; Hayes, S. E.; Bowman, R. C.; Conradi, M. S. NMR Study of Anion Dynamics in Solid $KAlH_4$. *J. Phys. Chem. C* **2014**, *118*, 5725−5732.
(34) Markert, J. T.; Cotts, E. J.; Cotts, R. M. Hydrogen Diffusion in the Metallic Glass a-$Zr_3RhH_{3.5}$. *Phys. Rev. B: Condens. Matter Mater. Phys.* **1988**, *37*, 6446−6452.
(35) Haupt, J. Einfluβ von Quanteneffekten der Methylgruppenrotation auf die Kernrelaxation in Festkörpern. *Z. Naturforsch., A: Phys. Sci.* **1971**, *26*, 1578−1589.
(36) Müller-Warmuth, W.; Schüler, R.; Prager, M.; Kollmar, A. Rotational Tunneling in Methylpyridines as Studied by NMR Relaxation and Inelastic Neutron Scattering. *J. Chem. Phys.* **1978**, *69*, 2382−2392.
(37) Prager, M.; Hempelmann, R.; Langen, H.; Müller-Warmuth, W. Methyl Tunneling and Rotational Potentials in Solid Xylenes and Fluorotoluenes. *J. Phys.: Condens. Matter* **1990**, *2*, 8625−8638.
(38) Ingman, L. P.; Punkkinen, M.; Vuorimäki, A. H.; Ylinen, E. E. Proton Spin-Lattice Relaxation and Ammonium Tunnelling in $(NH_4)_2ZnCl_4$. *J. Phys. C: Solid State Phys.* **1985**, *18*, 5033−5041.
(39) Svare, I. Proton Tunneling Frequencies in Ammonium Salts from Spin-Lattice Relaxation. *J. Phys. C: Solid State Phys.* **1977**, *10*, 4137−4147.

DOI: 10.1021/acs.jpcc.7b12046
J. Phys. Chem. C 2018, 122, 3256−3262